



# Chick embryonic cells as a source for generating in vitro model of muscle cell dystrophy

Verma Urja<sup>1</sup> · Kashmiri Khairi<sup>1</sup> · Suresh Balakrishnan<sup>1</sup> · Gowri Kumari Uggini<sup>1</sup>

Received: 4 July 2018 / Accepted: 19 September 2018 / Editor: Tetsuji Okamoto  
© The Society for In Vitro Biology 2018

## Abstract

Chick embryonic cells can be used to develop an easy and economical in vitro model for conducting studies on the disease muscle dystrophy (MD). For this, the limb myoblasts from 11th day chick embryo were isolated and cultured. To this muscle cell culture, anti-dystroglycan antibody (IIH6) was added so as to target the  $\alpha$ -dystroglycan and disrupt the connection between the cytoskeletal proteins and the extracellular matrix (which is a characteristic feature of MD). Cells were allowed to differentiate further and the morphometrics and mRNA expression were studied. The IIH6-treated muscle cells displayed changes in morphometry, contractibility, and also atrophy was observed when compared to the control cultures. Concomitant gene expression studies showed an upregulation in TGF- $\beta$  expression, while the muscle sculpture genes MYOD1, MYF5, LAMA2 and MYOG were downregulated resembling the MD in vivo. This simple and cost-effective method can be useful in studies to further understand the disease mechanism and also in conducting initial studies on effect of novel pharmacological agents.

**Keywords** Chick embryo · Embryonic cells · Muscle dystrophy · In vitro model ·  $\alpha$ -dystroglycan

## Introduction

The molecular players in development of vertebrate muscles are being studied since late 1980s. Myoblast determination protein 1 (MYOD1), myogenin (MYOG), myogenic factor 5 (MYF5) and Myogenic regulatory factor 4 (MRF4) are the earliest identified myogenic regulatory factors (Davis et al. 1987; Wright et al. 1989; Braun et al. 1989). The complete faction of factors leading to development of muscles during the embryonic development and maintenance as well as regeneration in case of post-embryonic development is still being researched. Ample evidence exist to suggest the fact that myogenesis is a conserved process in evolution, and all the vertebrates bear more or less similar structures and proteins at the muscle tissue level (Braun et al. 1989). Vertebrate sarcolemma contains an assembly of glycoproteins which include  $\alpha$  and  $\beta$  sub types of dystroglycan and  $\alpha$ ,  $\beta$  and  $\gamma$  sub types of sarcoglycan and dystrophin. The components of this complex when isolated and identified were found to be associated with dystrophin protein and

thus widely known as dystrophin-glycoprotein complex (Campbell and Kahl 1989). Any genetic modification leading to defect in gene expression or protein synthesis of any of the proteins of this complex leads to severe muscle developmental defects. Muscular dystrophy (MD) is one such disease leading to progressive muscle weakness and atrophy. Out of many variants of MDs, Duchenne muscular dystrophy (DMD) is the most commonly occurring (Emery et al. 2015; Theadom et al. 2014). It occurs due to a deletion, insertion, point mutation, duplication or similar genetic mutations in dystrophin gene (McGreevy et al. 2015).

The dystrophin and associated proteins provide mechanical strength to contracting muscles. They bind to cytoskeletal components of muscles and also help in signal transduction over muscle membranes. Any deviation from normal genetic structure of these proteins leads to an altered and/or defective gene expression and protein production. The resulting myofibres possess less strength and contractibility as well as regenerative capacity. Till date, an effective cure for MD is not known. The drugs are mainly targeted to the symptoms. Thus, MD remains to be an incurable, grave disorder which leads to the death of many people yearly, worldwide.

Basic biology of MD and clinical aspects of the disease in presence of drugs are studied mostly in mdx mice and cDMD dogs (McGreevy et al. 2015; Manning and

✉ Gowri Kumari Uggini  
uggini.gowri-zoo@msubaroda.ac.in

<sup>1</sup> Department of Zoology, Faculty of Science, The Maharaja Sayajirao University of Baroda, Vadodara 390002, India

O'Malley 2015). Use of stem cells from human and mice embryos as well as non-muscle cell types to induce muscle cell lines and later use them for induction of MD in vitro are well being considered (Salani et al. 2012). The disadvantages like ethical issues, longer range for obtaining myogenic cells in case of induced myogenic cell lines, change in genetic makeup of cells in case of transfection methods involved in induction of myogenesis, involvement of expensive factors for conversion and maintenance of these cells and insufficient amount of cells for sorting them are the major challenges in this field (Salani et al. 2012).

Myogenesis in chick progresses in a very similar way to humans. A major part of initial study on myogenesis in limbs and other organs were carried out in chick embryos (Masaki 1974; Dennis et al. 1984). The developing chick embryo has been a promising model for carrying out investigations in developmental biology, stem cell research as well as disease modelling. Chick embryos were even used as model systems for the study of cardiac development as well as disease (Hutson and Kirby 2007). Cultured chick embryo sympathetic neurons were used to study the pathogenetic mechanisms in Parkinson's disease (Ziv et al. 1994). The ease of manipulation, cost effectiveness and also a considerable degree of genetic resemblance with mammals has made its contributions more steadfast. Owing to these advantages, we used the skeletal muscle cells from chick embryo to develop an in vitro cell model for MD. There have been studies focussing on pathology of muscular dystrophy using dystrophic chick as model, wherein the role of sarcolemmal localization of WWP1 protein was established (Imamura et al. 2015). Identification of chicken muscular dystrophy dates back to 1950s (Asmundson and Julian 1956) while the histological changes in dystrophic chicken muscles were identified in late 1970s (Wilson et al. 1979). Here, we attempted to culture chick embryonic limb skeletal muscle cells and induce MD by means of antibody blockade of one of the important proteins in the dystrophin-associated sarcolemmal assembly,  $\alpha$ -dystroglycan. MD is known to be caused by mutations in the dystrophin gene, which is vital in maintaining the structural integrity of the muscle and its components. Dystroglycans are vital members of the skeletal muscle dystrophin-glycoprotein complex, as they link dystrophin to proteins in the extracellular matrix.  $\alpha$ -Dystroglycan is a receptor for laminin  $\alpha$ -2, an extracellular matrix protein which mediates cell attachment and tissue organisation (Henry and Campbell 1999). Further, human muscular dystrophy disorders have been shown to arise from defective glycosylation of the  $\alpha$ -dystroglycan subunit (Jimenez-Mallebrera et al. 2005). Therefore, in an effort to create a MD-like phenotype in the muscle cells in vitro, we tried to block the linkage between the dystrophin and laminin  $\alpha$ -2 in the cultured cells.

## Materials and Methods

**Source of embryonic cells** Freshly laid fertile RIR (Rhode Island Red) eggs of *Gallus domesticus* were procured from government intensive poultry farm, Vadodara. They were incubated at 37°C with 75% relative humidity and rotated every 2 h till the stage of isolation. The experimental protocols were approved by the Institutional Animal Ethics Committee (IAEC) in accordance with the Committee for the Purpose of Control and Supervision of Experiments on Animals (No. MSU-Z/IAEC/13-2017), India.

**Isolation of Chick Embryonic Skeletal Muscle Cells (cESMC)** cESMC were isolated from chick embryo at HH stage 37 (Hamburger and Hamilton 1951). All the procedures were carried out under laminar air flow hood. The embryo was isolated and taken into PBS (calcium-magnesium-free; autoclaved). All the four limbs were separated and washed so as to get rid of RBCs. Digits were removed. The limbs were deskinning with the help of blunt scalpel. The tissues were then put in 10 ml Dulbecco's modified Eagle medium (DMEM) with low glucose and pyruvate (Gibco, Life Technologies, Waltham, MA) in centrifuge tube. Ten per cent trypsin-EDTA (Gibco, Life Technologies) was added and tissue was minced with the help of autoclaved sterile scissors. This tube was incubated at 37°C in water bath for 10 min. Post-incubation, 10% trypsin neutralising solution (Gibco, Life Technologies) was added to the tube. The content was centrifuged at 1000 rpm at room temperature for 10 min to pellet down the cells and remove trypsin. Pellet was re-suspended in 10-ml media mix. Media mix contained DMEM-low glucose with 10% FBS (Gibco, Life Technologies) and 1× antibiotics (Gibco, Life Technologies). This prepared cell suspension was seeded onto a non-coated sterile culture vessel for 2 h allowing fibroblast cells to attach. Later, inspecting the attached fibroblast cells, media was isolated which contained majorly the muscle cells. These cells were counted and seeded in 60-mm tissue-culture-grade dishes (Tarsons, Kolkata, India).

**Cell count and plating** Cells were counted using haemocytometer by taking 10  $\mu$ l of cell suspension. Culture dishes were coated with 0.5% gelatine a day before seeding cells. The cells were plated at seeding density of  $2 \times 10^5$  cells per ml of media mix. The culture vessels were then put in CO<sub>2</sub> incubator without disturbance for minimum 6 h so that they get attached to the substratum.

**Antibody-mediated disruption of  $\alpha$ -dystroglycan linkage** The anti-dystroglycan antibody, IIH6 (DSHB, University of Iowa, Iowa City, IA), was used to target the  $\alpha$ -

dystroglycan and severe linkage between the dystrophin and laminin  $\alpha$ -2 in the cultured cESMC. Cells were divided into different groups: untreated control (UC), supernatant treated control (STC), isotype control (IC) and treatment group (T). The UC cells received no experimental treatment. The STC culture was treated with 10% supernatant alone of IIH6 Ab solution prepared by centrifugation of antibody solution mixed with 50% ammonium sulphate at 5000 rpm for 20 min at 4°C, so as to rule out any non-specific effects of antibody solution or the preservatives present in it (Grodzki and Berenstein 2010). The IC culture was treated with IgM isotype (Sigma-Aldrich, St. Louis, MO); the dose chosen was similar to that of the IIH6 Ab used in the T group. In the T group of culture, for initial standardisation of antibody blockade, different culture plates were added with the antibody on the third day of fusion and were tested with different concentrations of the antibody: 2.1, 1.05, 0.525 and 0.350  $\mu$ g/ml media mix.

**Trypan blue exclusion test** Ten microlitres media containing the detached cells from each group of cultured cells was taken for the test at the intervals of 8 h for 24 h post-treatment. From these cell suspensions, percentage non-viable cells were counted with the help of trypan blue exclusion test. Trypan blue (0.04%) (in PBS) was added in 1:1 ratio to collected cell suspension, and 10  $\mu$ l of this mixture was immediately taken on haemocytometer for calculating the ratio of dead (blue) vs. live (colourless) cells (Strober 2015). Values of percentage non-viable cells were further tested by performing two-way ANOVA (GraphPad Software Inc., La Jolla, CA).

Among all the antibody treatment doses, 0.525  $\mu$ g/ml concentration of the IIH6 antibody was selected for further observations, as the said dose seemed to induce morphological changes similar to dystrophic phenotype, and the cell deaths were relatively less. Media mix was not changed during differentiation phase. However, at every 48-h interval, media mix was added to compensate the loss of evaporated media.

**Myotube morphometry and contractibility** For morphometry, 12-well plates were seeded with cESMC for each of the UC, STC, IC and T group (0.525  $\mu$ g/ml). Further, three fields of view (under 10 $\times$  objective) were selected randomly from each well for counting numbers of myotubes. For widths, five randomly selected myotubes were considered per well. Myotube diameters were calculated by ISCapture software (Tucsen Photonics, China). One-way ANOVA was performed for understanding the significant deviation in average numbers and widths of myotubes of treated cultures relative to the control cultures.

Since there were no significant differences in the above two phenomena among the three control groups, all further experiments were carried with only two groups IC and T (0.525  $\mu$ g/ml). For testing the contractibility, 12-well plates were seeded with cells, treated (one with isotype control and one with IIH6) and grown till myotube stage; 80 mM KCl was added to each well at a time and time taken for starting the contractions in each was noted (Paulino et al. 2003). Independent sample *t* test was performed to look for any significant variation in the means of contraction times among the groups. After formation of myofibres, number of myofibres with normal and dystrophic phenotypes was calculated and plotted in a graph after performing Student's *t* test (GraphPad Software Inc.).

**LADD and DAPI staining** To understand whether the antibody blockade can hinder myoblast fusion, on the very day of seeding, the cells were set as IC and T groups. LADD multiple staining was done 3 days post-seeding according to the protocol described by Rhys McColl and co-workers (McColl et al. 2016). The cells were washed with PBS thrice to get rid of media and were fixed in 70% ethanol. Later, the stain was added at final volume of 500  $\mu$ l which was prepared from 0.50 g toluidine blue (Sigma-Aldrich) and 0.15 g fuchsin (Sigma-Aldrich) in a final volume of 100 ml of 30% ethanol. The cells were kept immersed in the stain for 5 min. Excess stain was removed with the help of PBS. All the culture plates were observed under phase-contrast inverted microscope (Lawrence and Mayo, Mumbai, India) LM-52-3501. Fusion index was calculated by counting cells undergoing fusion in ten fields (two from each well) under  $\times$ 20 objective view. The myoblast fusion was analysed by calculating fusion index [(percentage cells fusing/total cells in field) \* 100]. Data was analysed using independent-sample *t* test to identify significant mean differences. For DAPI staining, the cells were treated with 30 nM DAPI solution (prepared in PBS). Thirty minutes after adding this solution, the images were taken by Leica EZ camera. The staining procedure was carried out in dark.

**Detection of cell death by EtBr/AO staining** IC and T group cultures were seeded over a coverslip and washed with PBS twice to get rid of media completely. Coverslips were immersed in 1 ml PBS added with 80  $\mu$ l EtBr/Acridine orange mix prepared from 100  $\mu$ g/ml concentrations of each dye (Ribble et al. 2005). After 5 min of incubation, apoptotic cells (orange coloured) were scored under fluorescent microscope (Leica DM2500, Olympus, Tokyo, Japan). Images were taken by Leica EZ camera. Twenty fields were scored under  $\times$ 40 objective view and calculated percentage of apoptotic cells in each. Further,

Student's *t* test was performed to check the significant variation among the two groups.

**Cleaved caspase-3,  $\beta$ -dystroglycan and MyoD localization by immunostaining** The cells were seeded on APES-coated slides for immunocytochemistry. The whole protocol was carried out by keeping coverslips upright in the petri dishes of 35 mm diameter. Coverslips were rinsed with PBST and fixed with chilled methanol for 5 min. Then, they were washed thrice with PBS. Antigen retrieval was carried out by adding preheated retrieval buffer (100 mM Tris buffer in 5% Urea solution) at 95°C on the coverslips for 10 min. Again, three subsequent washes with PBS were given for 5 min each. The coverslips were then incubated with permeabilization buffer for 10 min at room temperature. Three PBS washes of 5 min each were given again. Blocking was performed by incubating in blocking buffer for 1 h at room temperature. The cells were incubated in primary monoclonal cleaved caspase-3 antibody (Sigma-Aldrich), diluted 1:500 in PBST, for 1 h at room temperature. For MyoD localisation, primary monoclonal antibody (DSHB, University of Iowa) was used. Primary anti- $\beta$ -dystroglycan (DSHB, University of Iowa) was diluted 50 times in PBST for its localization. Excess antibodies were removed by giving three PBS washes for 5 min each. Samples were then incubated in FITC-conjugated secondary goat anti-rabbit IgG antibody (Genei, Bangalore, India) diluted 200 times with PBST, for 1 h at room temperature in dark for cleaved caspase-3 localization. For MyoD and  $\beta$ -dystroglycan localisation, anti-mouse secondary antibody conjugated with FITC (Genei) was used. Excess antibodies were washed off by washing thrice (for 5 min each time) with PBS. The fluorescence was observed and captured with the help of fluorescent microscope and camera. Images were merged using ImageJ software.

**Western blot of cleaved caspase-3** Protein expression status of cleaved caspase-3 was checked by Western blot method. Protein was isolated from approx.  $10^8$  cells in the lysis buffer (50 mM Tris pH 7.5, 200 mM NaCl, 10 mM  $\text{CaCl}_2$  and 1% triton-X 100). The lysed mixture was centrifuged further at 12,000 rpm for 10 min, and the supernatant was then used for protein estimation done by Bradford method (Bradford, 1976). Thirty micrograms of protein was then allowed to electrophorese through SDS-PAGE, on 12% gel to separate the constituent proteins, which were then transferred on PVDF membrane by blotting method. The membrane was stained next, with Ponceau, to observe the quality of transfer and then subjected to cleaved caspase-3-specific primary antibody (Sigma-Aldrich), overnight. Further, following the

complete protocol of blotting and due to exposure to the secondary antibody (goat anti-rabbit IgG antibody, GeNei, India) that exhibited clear bands of protein, which were tested for their band intensities, using Doc-ItLs software (DBA Analytik Jena US, Upland, CA) and the obtained values were normalised with the corresponding  $\beta$ -actin band intensities.

**Gene expression patterns of MYOD1, TGFB1, MYF5, LAMA2 and MYOG** The UC, IC and T groups were separately harvested in TRIzol reagent (Invitrogen) at secondary myotube stage for RNA isolation. The process was followed by decanting media followed by PBS (calcium-magnesium-free) washing and then addition of TRIzol. Cells added with TRIzol were detached with the help of sterile cell scraper (Tarsons). Three dishes confluent with cells were utilised for RNA isolation in 1 ml TRIzol reagent. RNA was reverse transcribed to cDNA by High-Capacity cDNA Reverse Transcriptase Kit (Applied Biosystems, Foster City, CA) according to the manufacturer's instruction. These were screened for gene expression of MYOD1, TGFB1, MYF5, LAMA2 and MYOG with the help of polymerase chain reaction with an initial denaturation at 94°C for 3 min, followed by 32 cycles of 10 s at 94°C (denaturation), 20 s at 60°C (annealing) and 20 s at 72°C (extension). 18s rRNA was used as a house keeping gene. Following were the primer sequences:

MYOD1: fwd: CGGAATCACCAAATGACCCAA; rev: ATCTGGGCTCCACTGTCACT  
 TGFB1: fwd: TCGACTTCCGCAAGGATCTG; rev: CCCGGGTTGTGTTGGTTGTA  
 MYF5: fwd: CCAGGAGCTCTTGAGGGAAC; rev: AGTCCGCCATCACATCGGAG  
 LAMA2: fwd: TCCCCTCTTGATTCGTGTGC; rev: AAGCCAGAGTCAGCCATTGT  
 MYOG: fwd: CATCCAGTACATCGAGCGCC; rev: GCTCAGGAGGTGATCTGCC  
 18s rRNA: fwd: GGCCGTTCTTAGTTGGTGGA; rev: CAATCTCGGGTGGCTGAAC

**Real-time RT-PCR** Real-time Reverse Transcriptase PCR was performed on a Lightcycler96 (Roche Diagnostics, Basel, Switzerland) for MYOD1, TGFB1, MYF5, LAMA2 and MYOG to identify relative quantities of these in isotype-control cells and IIH6-treated cells. The program was set as follows: 3 min at 95°C, 35 cycles (each cycle of 10 s at 95°C, 10 s at 60°C and 10 s at 72°C). Melting curves for each well were used to confirm the specificity of the products. 18s rRNA was used as an internal loading control. Mean Cq values of control gene expressions were normalised with internal control gene

expression for each group (control and treated). Fold change in expression of both the genes compared to control group was calculated using  $2^{-\Delta\Delta C_q}$  values as described by Livak and Schmittgen (Livak and Schmittgen 2001). Data was analysed by Student's *t* test for significance of mean differences.

### Statistical operations

All the above mentioned statistical analysis was carried out using GraphPad Prism v5.03 (GraphPad Software Inc.).

## Results

**cESMC in vitro** The isolated and cultured embryonic skeletal muscle cells presented the typical myoblastic morphology with large cell bodies bearing multiple processes. These embryonic skeletal muscle cells proliferated and became confluent in 2 days when seeded at density of  $2 \times 10^5$  cells per ml. The fusion could be observed on the third or fourth day of plating (Figs. 1a–d and 2). Multiple nuclei were visible in the fusing cells which then transformed into long primary myotubes. Around 12 days post-fusion, multilayered secondary myofibres were differentiated.

**IIH6 antibody-mediated blockade of laminin  $\alpha 2$  and  $\alpha$ -dystroglycan** Addition of different concentrations of antibody led to

modulated severity of phenotypic abnormalities. For the T group, 0.525  $\mu\text{g}/\text{ml}$  was finalised based on the following results.

**Trypan blue exclusion test** All the selected concentrations of IIH6 treatment caused significant cell death in cultured cESMCs. IIH6 (2.1  $\mu\text{g}/\text{ml}$ ) caused more than 50% mortality in the duration of 24 h of treatment. This fast progression of cell death is not ideal for the model system of dystrophy as increasing cell death evokes immediate inflammation and early breakdown of an in vitro system, making it of no use for further experimentation. About 50% cells became non-viable in second treatment group with 1.05  $\mu\text{g}/\text{ml}$  IIH6, making it unsuitable again. The next two doses decreased viability in a gradual manner and nearly 10% or less cells died in a day's time. The lowest concentration caused too less mortality. Therefore, the T group was set to receive 0.525  $\mu\text{g}/\text{ml}$  concentration. The cell deaths recorded in all the different doses of the T group were significantly higher than that in the IC group given 2.1  $\mu\text{g}/\text{ml}$  of IgM isotype antibody (Fig. 2).

**Myotube morphometry and contractibility** Both myotube numbers and widths showed that the selected dose of IIH6 caused significant changes in morphological features of the cultured cESMCs. Average number of myotubes was found to be around 11 in UC, STC and IC cultures while in the T group, the number was significantly reduced ( $***p \leq 0.001$ ) (Fig. 3). Mean myotube widths of T group cultures showed statistically no significant variation relative to the controls (Fig. 4);

**Figure 1.** Control morphology of cultured chicken embryonic skeletal muscle cells. **a** A typical fibroblastic morphology of substratum-anchored cells seen in phase-contrast microscopy-based  $\times 100$  field view (day 1), scale 200  $\mu\text{m}$ . **b** Myogenic cells fusing for formation of primary myotubes (day 4), scale 200  $\mu\text{m}$ . **c** Differentiating cells forming secondary myofibres (day 10), scale 100  $\mu\text{m}$ . **d** Morphology of myofibre in control culture, scale 100  $\mu\text{m}$ .

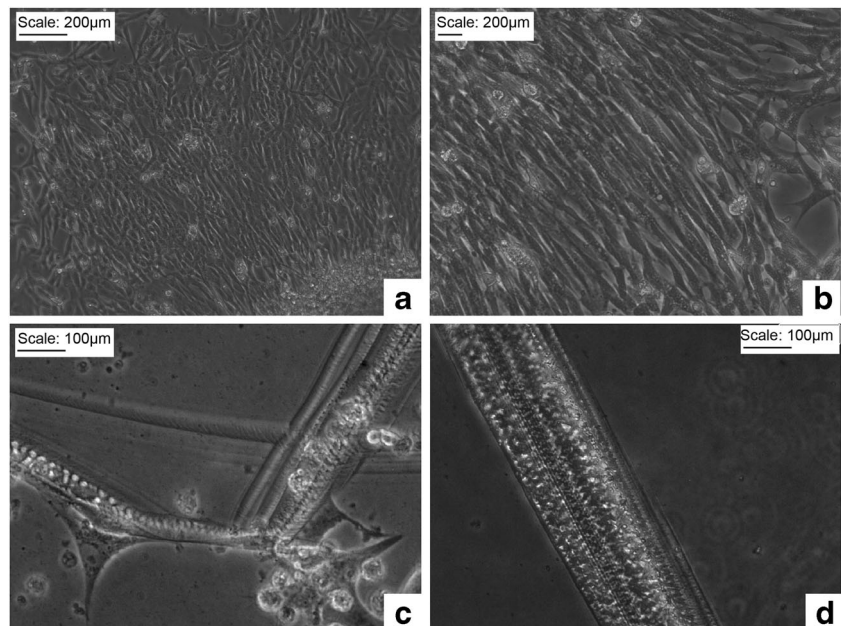
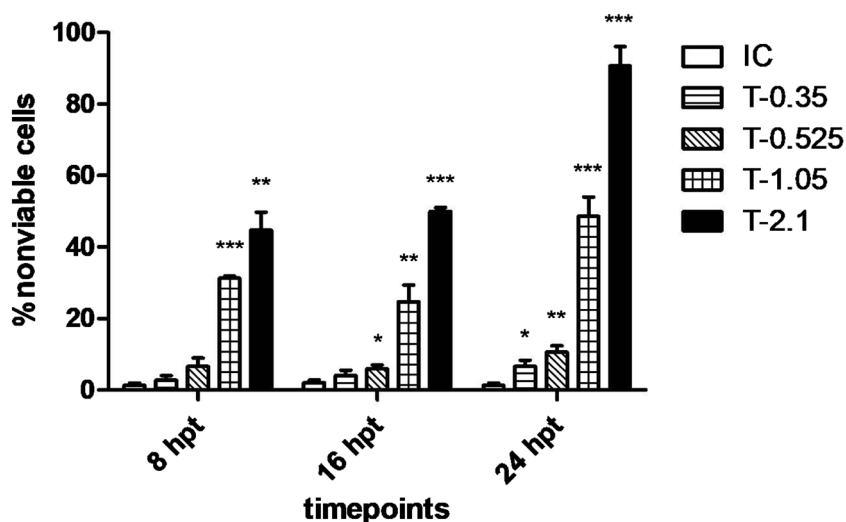


**Figure 2.** Percentage non-viable cells in various treatment groups viz. isotype control, 0.35, 0.525, 1.05 and 2.1  $\mu\text{g/ml}$  doses of IIH6. \* $p \leq 0.05$ ; \*\* $p \leq 0.01$ ; \*\*\* $p \leq 0.001$ . hpt—hours post-treatment.



however, there was an aberrance observed among the myotubes of T group where the upper and lower limits of myotube diameters showed noticeable variations.

While testing the contractility, addition of KCl to the culture media led to spontaneous contraction of cells in less than 20 s in all the UC, STC and IC culture wells. The T group deferred showing a highly significant decrease in the contraction time (\*\* $p \leq 0.001$ ) (Fig. 5).

Seven to eight days post-fusion, the morphology of myofibres in the T group showed very evident alterations which included wavy margins, splitting in between and at the ends of myofibres, breakage, damage, bifurcations and heavy cell death, while such changes were not observed in the control phenotypes (Fig. 6a–g). Typically, the myofibres also lost the normally seen directionality while growing (Fig. 6h, i). Percentage of cells bearing normal

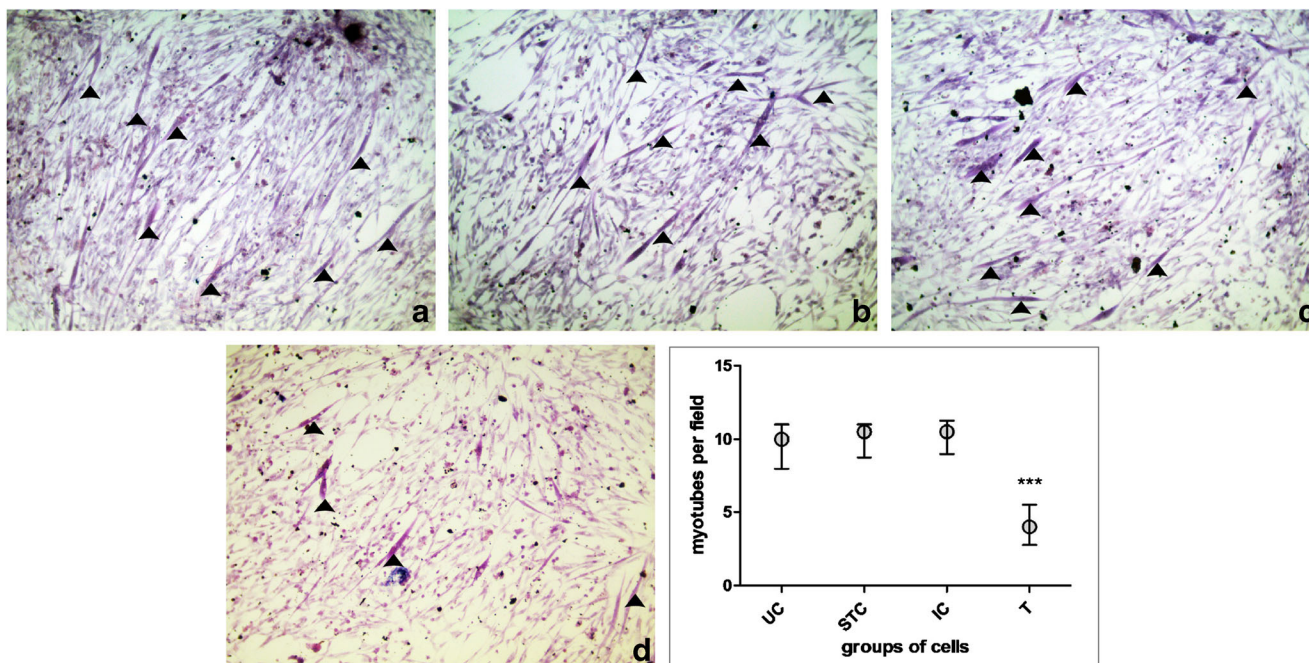


**Figure 3.** Variation in myotube numbers. Black arrowheads point at the myotube in each of the images. (a)  $\times 100$  field view of UC group with numerous myotubes stained with LADD for ease of evaluation. (b) Representative view from one of the culture vessels treated with supernatant of IIH6 (STC group) showing number of myotubes per view. (c) Cells of IC group showing abundant myotubes. (d)

Remarkable reduction in numbers of myotubes in treated cells. Graph: The values when analysed by performing one-way ANOVA showed that only treated cells had significantly less numbers of myotubes per field. There was no significant difference among all the control groups. \*\*\* $p \leq 0.001$ .

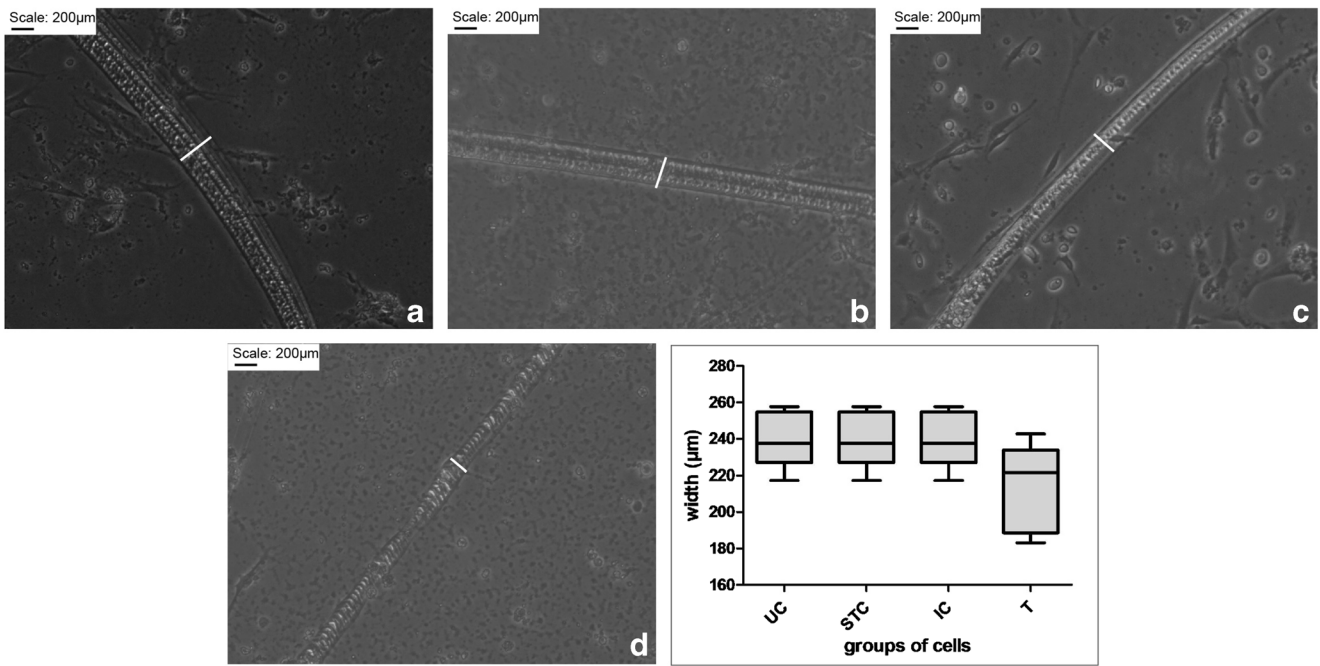


**Figure 4.** Myotube widths. Each of the **a–d** images are representing the normal phenotypic diameter of myofibres grown in the cESMC cultures belonging to UC, STC, IC and T respectively. Graph: The diameter values are plotted along with mean in the box plot. High internal variation in

widths of treated myotubes led to insignificant difference in mean of treated vs. control cultures. However, such variation is characteristic of MD condition.

morphology reduced in the treated group significantly (Fig. 6j).

**LADD and DAPI staining**

The LADD staining enabled a clear visualisation of the cell status, where the IC group showed a clear fusion of myoblasts into myotubes with multinucleate condition (Fig. 7a, c). The T group showed fewer numbers of

myoblasts fusing into myotubes and most of the cells being in uninucleate condition (Fig. 7b, d). The Fusion index of the T group cells showed a sharp decline, relative to the IC group ( $***p \leq 0.001$ ) (Fig. 7e). Multinucleation of fused myocytes was distinct in IC group whereas the T group showed separate cells. This was evident when the cells were stained with a nuclear stain DAPI (Fig. 7f).

**Detection of cell death by EtBr/AO staining**

Analysis by fluorescence-based technique showed that the T group cells showed characteristic dystrophic cell death. At primary myotube stage, the T group showed both the apoptosis and necrosis, visible by red and orange fluorescence respectively (Fig. 8a–f). When apoptotic and total number of cells were counted, it was found that about 30% cells were seen to be apoptotic on an average in T group while the apoptotic index was below 10% in IC group (Fig. 8b).

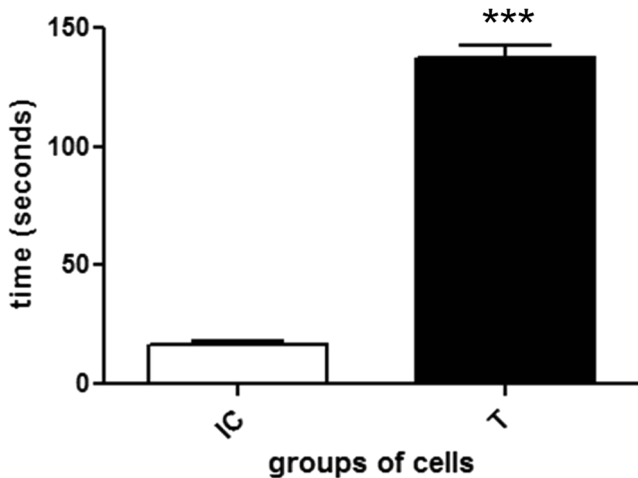


**Figure 5.** Time taken by cultures for exhibiting contraction.  $***p \leq 0.001$ .

**Cleaved caspase-3,  $\beta$ -dystroglycan and MyoD1 localization by immunostaining**

Localization of cleaved caspase-3 through immunostaining in the treated cells further supported the earlier result indicating that blocking dystroglycan can switch on apoptotic pathway during early myogenesis. Large amount

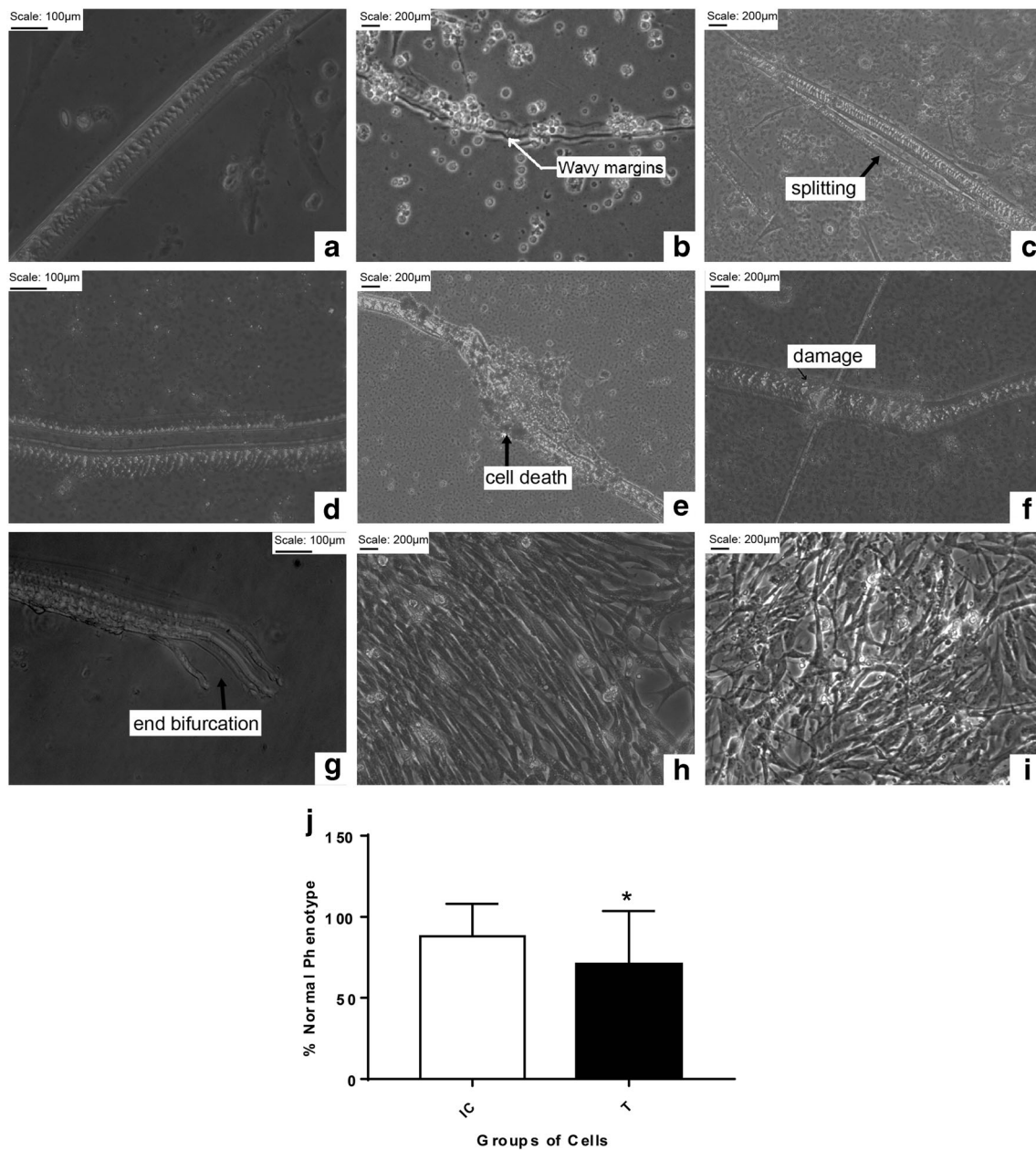


**Figure 6.** Morphological features of IC and T cultures. (a) Control morphology at  $\times 400$  magnification, scale 100  $\mu\text{m}$ . (b) Wavy margins of myotubes formed in treated culture, scale 200  $\mu\text{m}$ . (c) Central splitting in developed myofibre of treated culture, scale 200  $\mu\text{m}$ . (d) Disruption along sarcolemma of myofibre in treated culture, scale 200  $\mu\text{m}$ . (e) Cell death in treated myotube, scale 200  $\mu\text{m}$ . (f) Myofibre damaged along its length in treatment group, scale 200  $\mu\text{m}$ . (g) Treated

myofibre end-splitting, scale 200  $\mu\text{m}$ . (h) IC group cells showing normal morphology of myotubes growing in a unidirectional manner, scale 200  $\mu\text{m}$ . (i) Treated myotubes growing in various directions unlike normal growth, scale 200  $\mu\text{m}$ . (j) Graph showing the reduction in normal phenotype of myotubes in treated group when compared to isotype control.  $*p \leq 0.05$ .

of cells showed the presence of cleaved caspase-3 which adduced the atrophic state in T group compared to the control (Fig. 9). There were fewer signals from cells for protein MyoD1 in treatment when compared to control groups at the stage when fusion starts (Fig. 10). This is the stage when MyoD1 gets highest expressed in these cells (Abmayr and Pavlath 2012).  $\beta$ -Dystroglycan

localization revealed that unlike control cells, the treated myocytes showed decreased immunofluorescence.  $\beta$ -dystroglycan is known to be held at cell membrane by  $\alpha$ -dystroglycan which further connects to laminin. Blockage of laminin and  $\alpha$ -dystroglycan bond seems to cause delocalization of  $\beta$ -dystroglycan in the treated myocytes (Fig. 11).

**Western blot analysis of cleaved caspase-3** The Western blot analysis for cleaved caspase-3 shows significant increase in expression under the effect of the treatment. This is in accordance with the localisation results, further enforcing the results obtained.

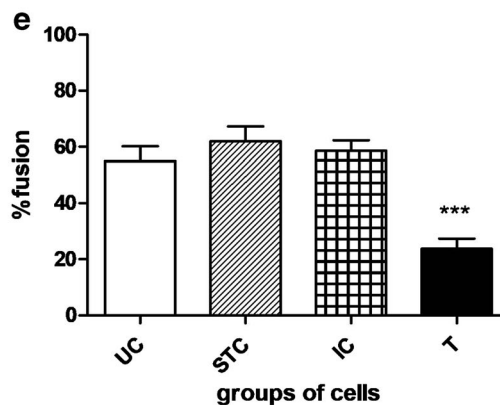
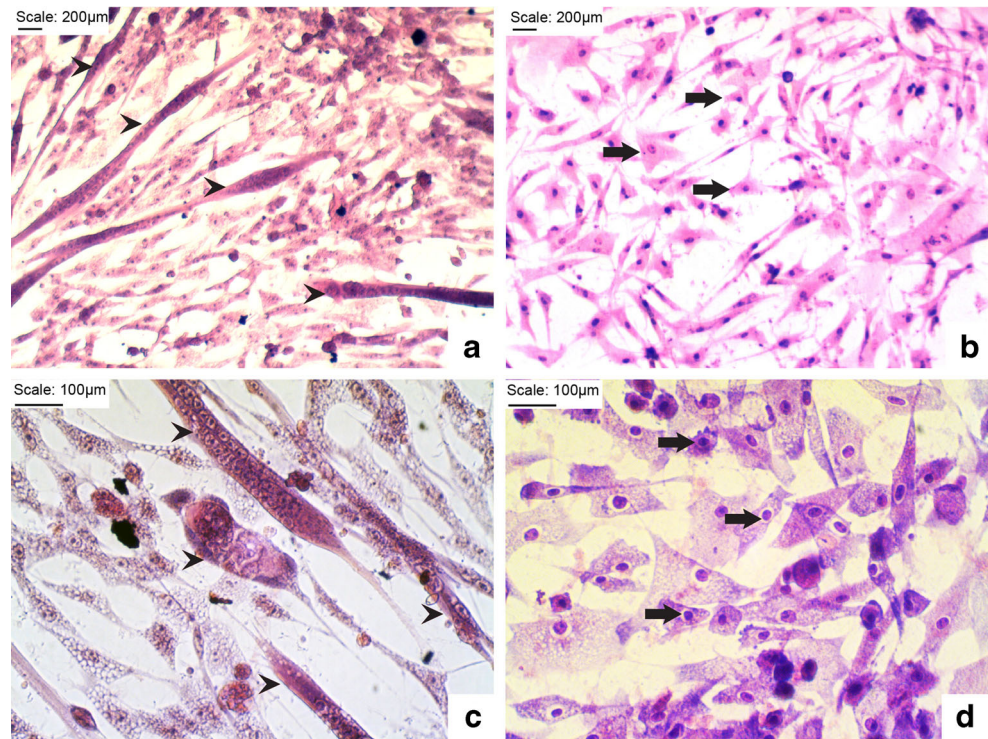
**Gene expression patterns of MYOD1, TGFB1, MYF5, LAMA2 and MYOG** While looking for the expression pattern of the characteristic dystrophic genes in the primary myotubes of control and treated cultures, we found an upregulation of TGFB1 levels in T group relative to the IC. Also, a sharp downregulation of genes related to muscle sculpture MYOD1, MYF5, LAMA2 and MYOG was noticed in the T group (Fig. 12). The control muscle cells contained high level

of LAMA2 which was diminished by 0.05-fold in the treated group. There were 0.009-, 0.5- and 0.06-fold reduction in the levels of MYOD1, MYF5 and MYOG respectively in the T group compared to the IC group (Fig. 12).

## Discussion

The development of the complex muscle tissue at the molecular level has been studied with the help of various animal models like *Drosophila*, Zebra fish, chick and mouse (Nunes et al. 2005). Use of chick as model to study myogenesis has a long history in developmental biology research (Masaki 1974; Dennis et al. 1984). The chick

**Figure 7.** LADD-stained control and treated cells. (a, c) Images represent control group with majority of cells undergoing fusion. The *arrowheads* show the formed myotubes with typical lighter multinuclei of fusing cells bearing darkly stained cytoplasm. (b, d) Images represent the treated cultures wherein *arrows* show dark nuclei of cells in lightly stained cytoplasm. Scale 200  $\mu\text{m}$  for a and b; 100  $\mu\text{m}$  for other images in the panel. (e) Fusion index calculated on the basis of LADD staining shows the heavy reduction in fusing cell numbers in treated group when compared to all other groups which show no significance differences among themselves.  $***p \leq 0.001$ . (f) DAPI staining for fusing cells of IC group and separate cells of treated culture, scale 100 px.



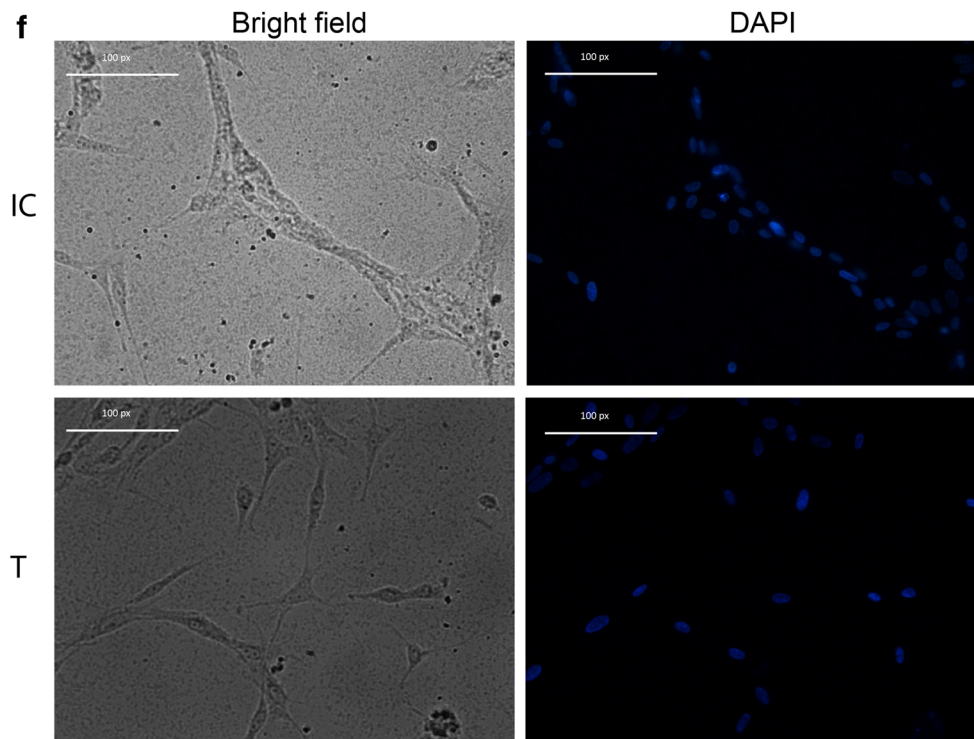


**Figure 7.** (continued)

embryonic skeletal muscle cells were used as an in vitro model to study the effect of vitamin E in prevention of cell death (Nunes et al. 2005). An earlier report described the method for isolation and culture of muscle cells from breast regions of developing chick (Godinho 2006). Here, we attempted to culture in vitro the muscle cells which could feature the condition of muscle dystrophy. The source was chick embryonic cells which gave the advantages of ease of availability, collection and manipulation of cells. The blockade of the connection between the extracellular matrix and cytoskeletal proteins of muscles by antibody IIIH6 lead to impairment of the connection between dystrophin and laminin, which resulted in the muscle cells, phenotypically similar to dystrophic muscle. A similar method of alteration of muscle cell morphology was earlier shown in the mouse skeletal muscle cells (Brown et al. 1999).

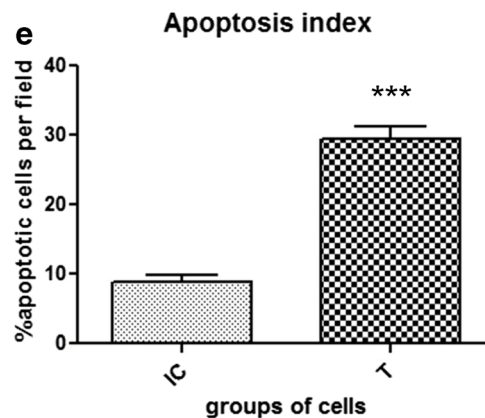
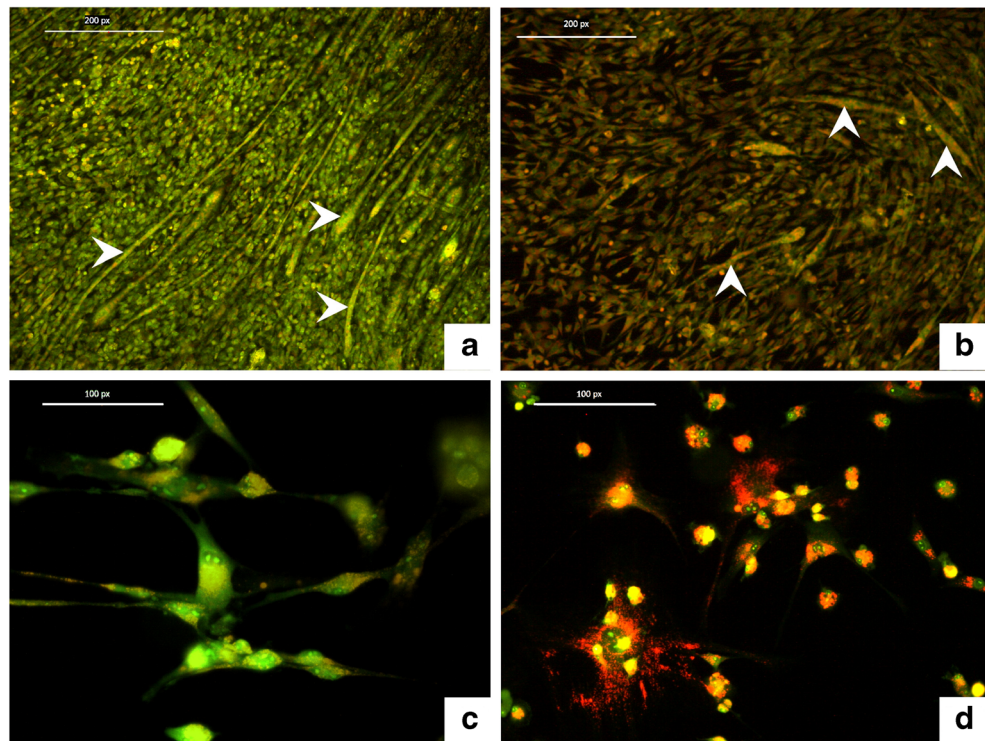
The phenotype of the targeted and cultured cells in the current experiment showed morphological variations similar to the MD condition in vivo or in few other animal models for MD: i.e. similar muscle cell phenotype was reported in patients suffering from muscle dystrophy (Isaacs et al. 1973; Schmalbruch 1976). Also, similar decrease in number and diameter as well as splitting of the myofibres was also observed in the dystrophic mice derived myofibres (Hernández-Ochoa et al. 2015). The variations observed in the diameter and the huge upper and lower limit differences are characteristic features of

dystrophic muscles. Thinner and few myotubes is the characteristic feature of dystrophy in vivo as well. These thinner and fewer myotubes might as well be responsible for impaired signal transmission and contraction. Our model also showed cell death and clumps of the dead cells in between the growing myofibres, disrupted basement membrane and multi-directional myofibres—the typical characters of myopathies as described in earlier reports (Williamson et al. 1997; Brown et al. 1999).

Further in an earlier in vitro study, the muscle cells from the hind limb of mice when treated with IIIH6 antibody to target  $\alpha$ -dystroglycan, it was reported that the procedure did not affect the fusion or myotube formation process and showed no indications of apoptosis till 7 d post-fusion (Brown et al. 1999). In contrary, we observed that the formation of myotubes was delayed and high level of apoptosis was induced by the blockade of  $\alpha$ -dystroglycan within 3 to 7 d of fusion process. There was almost 50% decrease in proportion of the cells undergoing fusion in treated cells when compared to control. This observation accentuates the role of  $\alpha$ -dystroglycan in initial myogenesis in the chick embryo and further, the above varied observation might even indicate variations in activation of specific molecular pathways in different species as well.

Laminin  $\alpha$ -2 is an extracellular matrix protein and is known to hold the muscle tissue integrity by reconciling

**Figure 8.** EtBr/AO staining in IC vs. T cells. **(a, c)** show control cells with minimum amount of apoptotic orange fluorescence and maximum amount of viable green phenotype. **(b, d)** show high amount of cells exhibiting apoptotic and necrotic phenotype. First and second row of images are  $\times 200$  and  $\times 400$  field views respectively. White *arrowheads* specifically mark the myotubes in normal **(a)** and apoptotic **(b)** states. **(g)** Apoptotic index in IC and T groups exhibiting typical rise in apoptotic cells in developed model system.  $***p \leq 0.001$ .

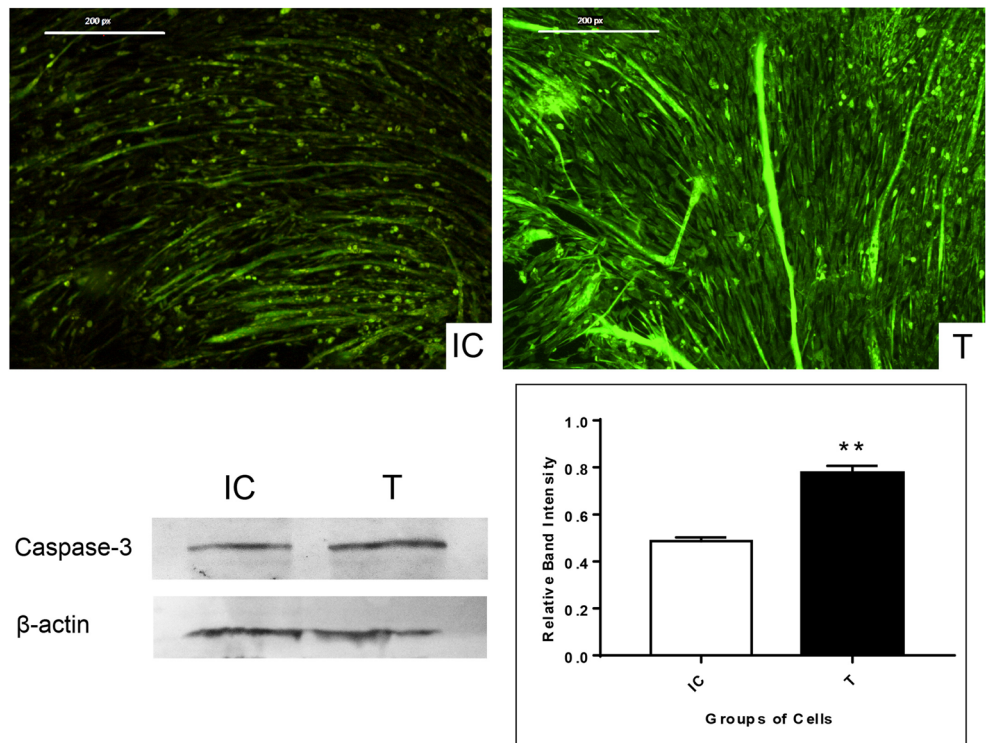


the attachment and organisation of the cells. A deficiency of laminin  $\alpha$ -2 was found to be typical to most of the cases of muscle dystrophy (Jimenez-Mallebrera et al. 2005). In concurrence to this occurrence, in our experiment, the dystrophied-like cells in vitro showed a decreased expression of LAMA2 gene. Additionally, our study showed an increase in the expression level of TGF- $\beta$ , which is a known regulator of fibrosis and inflammation. Muscles from DMD patients are known to express more TGF- $\beta$ , which stimulates the myoblasts to form myofibroblasts (Li et al. 2004). The heightened levels of TGF- $\beta$ , extra cellular matrix components get deposited, resulting in fibrotic changes and damage to membrane integrity of the muscle cell. Our model showed rise in the level of TGF $\beta$ 1 gene as well. Two other genes,

MYOD1 and MYOG, which got modulated by IHH6 treatment in our model, are widely known to regulate cell numbers and differentiation in muscle cells. In case of reprogramming during myogenic regeneration, MYOD1 gene remains upregulated in these tissues (Bentzinger et al. 2012).

Disorganisation of costameres in case of dystrophin gene defects are known to cause the inappropriate ROS generation and membrane leaks (Goldstein and McNally 2010). Our results showed that several of the dystrophy-induced myofibres ruptured at various points along the lengths. Similar descriptions were reported earlier, where even low-level mechanical pressure could bring about the membrane rupture in case of dystrophy (Friedrich et al. 2008; Biondi et al. 2013).

**Figure 9.** Immunolocalization of cleaved caspase-3 in control and treated cells. The treated myotubes intensively stained with cleaved caspase-3 antibodies when compared to control myotubes.  $\times 100$  field view, scale 200 px. Western blots of cleaved caspase-3 relative to the internal control  $\beta$ -actin showed significant increase of cleaved caspase-3 in treated cells when compared to control.  $**p \leq 0.01$ .



Currently available models including mdx mice are known to exhibit different disease progression than that in human at both phenotypic and molecular level. Moreover, there are alternative pathways like the utrophin

upregulation when dystrophin is knocked off in mice (McGreevy et al. 2015). Even the closely related model GRMD was found to escape from disease progression via Jagged1-Notch pathway (Vieira et al. 2015). The above

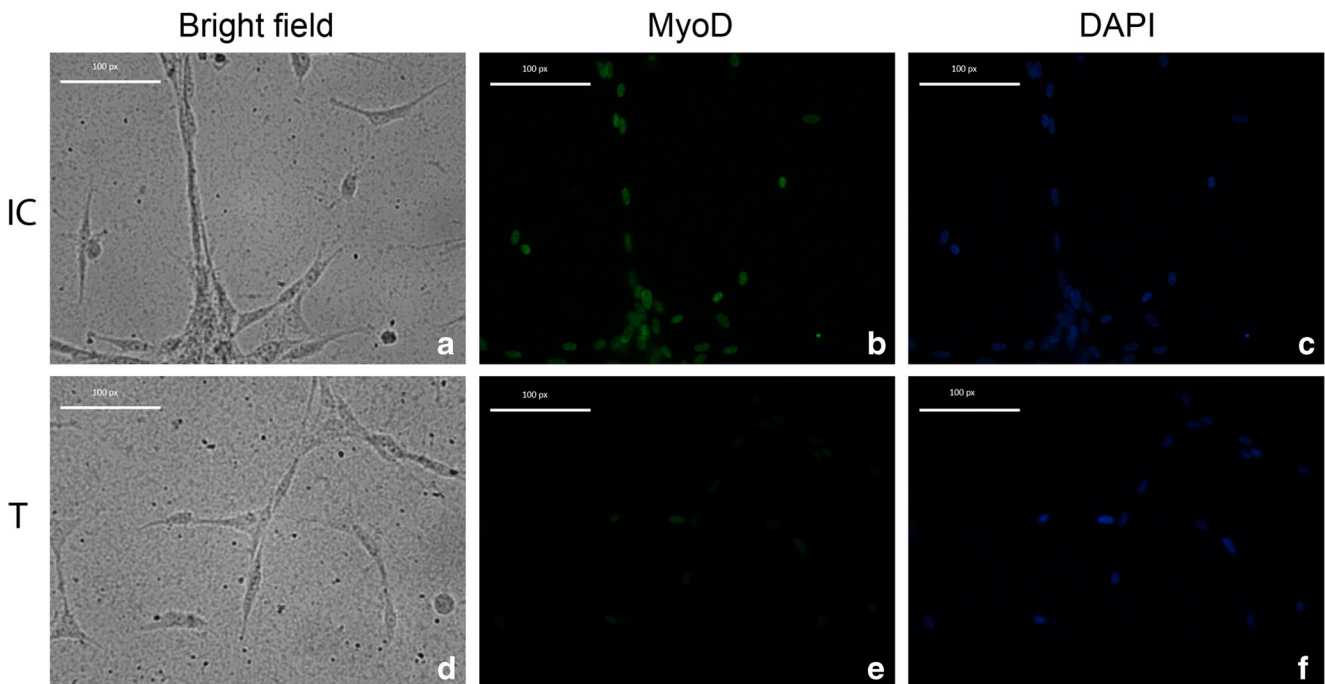


**Figure 10.** Immunolocalization of MyoD1 protein in IC vs T group. The upper panel (a–c) shows the control cells stained brightly with MyoD antibodies. The lower panel comprising of d–f show treatment group

cells wherein very few cells have got immunostained with MyoD antibody.  $\times 400$  field view, scale 100 px for each image.

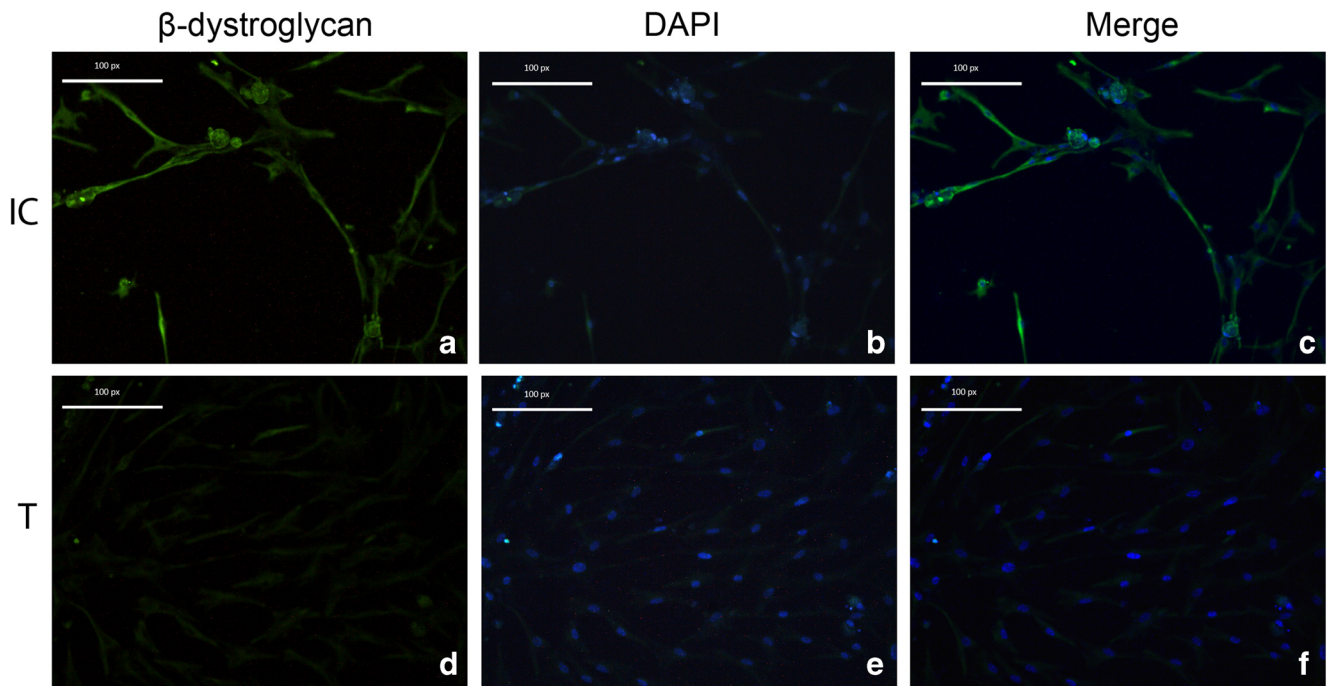


**Figure 11.** Immunolocalization of  $\beta$ -dystroglycan. The upper panel (a–c) includes control cells which have caught the staining intensively more than the treated cells placed in lower panel (d–f). b, e are respective counterstained images for a, d cells. Scale 100 px.

cases show how different species can evade the dystrophic condition even in absence of dystrophin gene mutations, unlike human.

Collectively, all the above-discussed models to muscle dystrophy have been quite efficiently able to analyse the disease pathology at various level; nevertheless, there remains a limitation. Among all these, the cells from the chick embryo as discussed here can be manipulated to resemble the muscle dystrophy condition in vitro with much ease and involves minimal animal sacrifice and ethical concerns. The morphological alterations, contractibility, atrophy and gene expression of the altered in vitro muscle cells we report here share

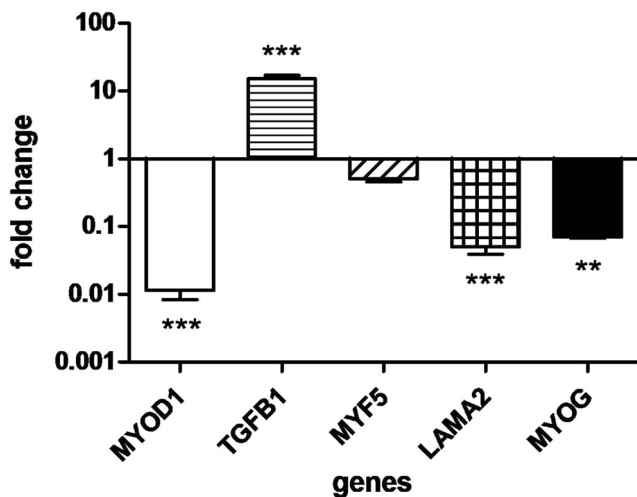


**Figure 12.** Quantitative difference in gene expression pattern between control and treated groups. \*\* $p \leq 0.01$ ; \*\*\* $p \leq 0.001$ .

high similarities to the MD condition. It could be an efficient model with low cost of development and maintenance, as it does not need many expensive growth factors and regulators. Owing to these advantages, we believe that these MD-like cell culture systems would be helpful in bringing further advancement in understanding the early molecular changes of this disease and also during preliminary drug evaluation.

### Conclusion

Chick embryonic muscle cells differentiate like human myogenic cells in vitro and in this course of endeavour, we developed ablation of Dystroglycan-Laminin bridge, via IHH6 treatment, which causes dystrophic cell phenotype and death. The developed model shows distorted gene expression pattern similar to MD models and is an economical and reliable alternative for preclinical evaluations.

**Funding** This work was supported by University Grants Commission, New Delhi, grant number F.No.43–593/2014(SR).

### References

Abmayr SM, Pavlath GK (2012) Myoblast fusion: lessons from flies and mice. *Development* 139(4):641–656

Asmundson VS, Julian LM (1956) Inherited muscle abnormality in the domestic fowl. *J Heredity* 47(5):248–252

- Bentzinger CF, Wang YX, Rudnicki MA (2012) Building muscle: molecular regulation of myogenesis. *Cold Spring Harb Perspect Biol* 4(2):a008342
- Biondi O, Villemeur M, Marchand A, Chretien F, Bourg N, Gherardi RK, Richard I, Authier FJ (2013) Dual effects of exercise in dysferlinopathy. *Am J Pathol* 182(6):2298–2309
- Bradford MM (1976) A rapid and sensitive method for the quantitation of microgram quantities of protein utilizing the principle of protein-dye binding. *Anal Biochem* 72(1–2):248–254
- Braun T, Bober E, Buschhausen-Denker G, Kohtz S, Grzeschik KH, Arnold HH, Kotz S (1989) Differential expression of myogenic determination genes in muscle cells: possible autoactivation by the Myf gene products. *The EMBO J* 8(12):3617–3625
- Brown SC, Fassati A, Popplewell L, Page AM, Henry MD, Campbell KP, Dickson G (1999) Dystrophic phenotype induced in vitro by antibody blockade of muscle alpha-dystroglycan-laminin interaction. *J Cell Sci* 112(2):209–216
- Campbell KP, Kahl SD (1989) Association of dystrophin and an integral membrane glycoprotein. *Nature* 338(6212):259–262
- Davis RL, Weintraub H, Lassar AB (1987) Expression of a single transfected cDNA converts fibroblasts to myoblasts. *Cell* 51(6):987–1000
- Dennis JE, Shimizu T, Reinach FC, Fischman DA (1984) Localization of C-protein isoforms in chicken skeletal muscle: ultrastructural detection using monoclonal antibodies. *The J Cell Biol* 98(4):1514–1522
- Emery AE, Muntoni F, Quinlivan RC (2015) Duchenne muscular dystrophy. OUP Oxford, England UK
- Friedrich O, Von Wegner F, Chamberlain JS, Fink RH, Rohrbach P (2008) L-type Ca<sup>2+</sup> channel function is linked to dystrophin expression in mammalian muscle. *PLoS One* 3(3):e1762
- Grodzki AC, Berenstein E (2010) antibody purification: affinity chromatography—protein a and protein G Sepharose. In: *Immunocytochemical methods and protocols*. Humana Press, New York, United States, pp 33–41
- Godinho RO (2006) In vitro development of skeletal muscle fiber. *Braz J Morphol Sci* 23:173–186
- Goldstein JA, McNally EM (2010) Mechanisms of muscle weakness in muscular dystrophy. *J Gen Physiol* 136(1):29–34
- Hamburger V, Hamilton HL (1951) A series of normal stages in the development of the chick embryo. *J Morphol* 88(1):49–92
- Henry MD, Campbell KP (1999) Dystroglycan inside and out. *Curr Opin Cell Biol* 11(5):602–607
- Hernández-Ochoa EO, Pratt SJ, Garcia-Pelagio KP, Schneider MF, Lovering RM (2015) Disruption of action potential and calcium signaling properties in malformed myofibers from dystrophin-deficient mice. *Physiol Rep* 3(4)
- Hutson MR, Kirby ML (2007) Model systems for the study of heart development and disease: cardiac neural crest and conotruncal malformations. *Semin Cell Dev Biol* 18(1):101–110
- Imamura M, Nakamura A, Mannen H, Takeda SI (2015) Characterization of WWP1 protein expression in skeletal muscle of muscular dystrophy chickens. *J Biochem* 159(2):171–179
- Isaacs ER, Bradley WG, Henderson G (1973) Longitudinal fibre splitting in muscular dystrophy: a serial cinematographic study. *J Neurol Neurosurg Psychiatry* 36(5):813–819
- Jimenez-Mallebrera C, Brown SC, Sewry CA, Muntoni F (2005) Congenital muscular dystrophy: molecular and cellular aspects. *Cell Mol Life Sci* 62(7–8):809–823
- Li Y, Foster W, Deasy BM, Chan Y, Prisk V, Tang Y, Cummins J, Huard J (2004) Transforming growth factor- $\beta$ 1 induces the differentiation of myogenic cells into fibrotic cells in injured skeletal muscle: a key event in muscle fibrogenesis. *Am J Pathol* 164(3):1007–1019
- Livak KJ, Schmittgen TD (2001) Analysis of relative gene expression data using real-time quantitative PCR and the 2<sup>-</sup>  $\Delta\Delta$ CT method. *Methods* 25(4):402–408
- Manning J, O'Malley D (2015) What has the mdx mouse model of duchenne muscular dystrophy contributed to our understanding of this disease? *J Muscle Res Cell Motil* 36(2):155–167
- Masaki T (1974) Immunochemical comparison of myosins from chicken cardiac, fast white, slow red, and smooth muscle. *J Biochem* 76(2):441–449
- McColl R, Nkosi M, Snyman C, Niesler C (2016) Analysis and quantification of in vitro myoblast fusion using the LADD multiple stain. *Biotechniques* 61:323–326
- McGreevy JW, Hakim CH, McIntosh MA, Duan D (2015) Animal models of Duchenne muscular dystrophy: from basic mechanisms to gene therapy. *Dis Model Mech* 8(3):195–213
- Nunes VA, Gozzo AJ, Cruz-Silva I, Juliano MA, Viel TA, Godinho RO, Meirelles FV, Sampaio MU, Sampaio CA, Araujo MS (2005) Vitamin E prevents cell death induced by mild oxidative stress in chicken skeletal muscle cells. *Comp Biochem Physiol C Toxicol Pharmacol* 141(3):225–240
- Paulino N, Dantas AP, Bankova V, Longhi DT, Scremin A, de Castro SL, Calixto JB (2003) Bulgarian propolis induces analgesic and anti-inflammatory effects in mice and inhibits in vitro contraction of airway smooth muscle. *J Pharmacol Sci* 93(3):307–313
- Ribble D, Goldstein NB, Norris DA, Shellman YG (2005) A simple technique for quantifying apoptosis in 96-well plates. *BMC Biotechnol* 5(1):12
- Salani S, Donadoni C, Rizzo F, Bresolin N, Comi GP, Corti S (2012) Generation of skeletal muscle cells from embryonic and induced pluripotent stem cells as an in vitro model and for therapy of muscular dystrophies. *J Cell Mol Med* 16(7):1353–1364
- Schmalbruch H (1976) Muscle fibre splitting and regeneration in diseased human muscle. *Neuropathol Appl Neurobiol* 2(1):3–19
- Strober W (2015) Trypan blue exclusion test of cell viability. *Curr Protoc Immunol* 111(1):A3-B
- Theadom A, Rodrigues M, Roxburgh R, Balalla S, Higgins C, Bhattacharjee R, Jones K, Krishnamurthi R, Feigin V (2014) Prevalence of muscular dystrophies: a systematic literature review. *Neuroepidemiology* 43(3–4):259–268
- Vieira NM, Elvers I, Alexander MS, Moreira YB, Eran A, Gomes JP, Marshall JL, Karlsson EK, Verjovski-Almeida S, Lindblad-Toh K, Kunkel LM (2015) Jagged 1 rescues the Duchenne muscular dystrophy phenotype. *Cell* 163(5):1204–1213
- Williamson RA, Henry MD, Daniels KJ, Hrstka RF, Lee JC, Sunada Y, Ibraghimov-Beskrovnaya O, Campbell KP (1997) Dystroglycan is essential for early embryonic development: disruption of Reichert's membrane in Dag1-null mice. *Hum Mol Genet* 6(6):831–841
- Wilson BW, Randall WR, Patterson GT, Entrikin RK (1979) Major physiologic and histochemical characteristics of inherited dystrophy of the chicken. *Ann N Y Acad Sci* 317(1):224–246
- Wright WE, Sassoon DA, Lin VK (1989) Myogenin, a factor regulating myogenesis, has a domain homologous to MyoD. *Cell* 56(4):607–617
- Ziv I, Melamed E, Nardi N, Luria D, Achiron A, Offen D, Barzilai A (1994) Dopamine induces apoptosis-like cell death in cultured chick sympathetic neurons—a possible novel pathogenetic mechanism in Parkinson's disease. *Neurosci Lett* 170(1):136–140